# Supplementary information

**Gallium nitride nanowire as a linker of molybdenum sulfides and silicon for photoelectrocatalytic water splitting**

Zhou et al.

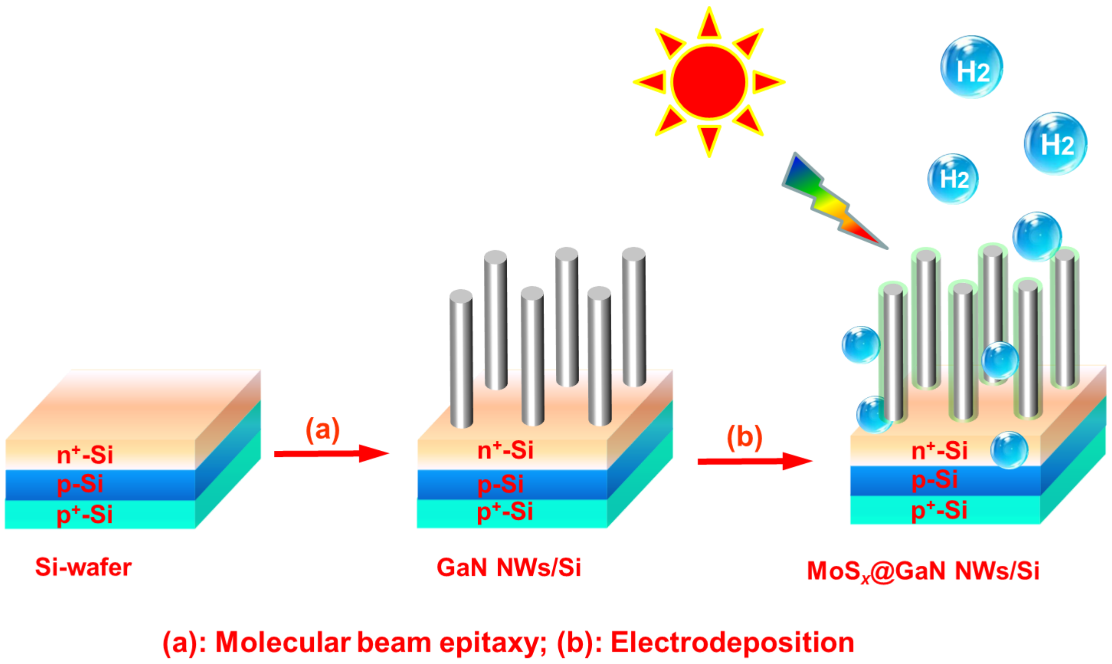


**Supplementary Figure 1** | Fabrication of shell-core $MoS_x$@GaN NWs/Si by molecular beam epitaxy and electrodeposition for solar water splitting to hydrogen.

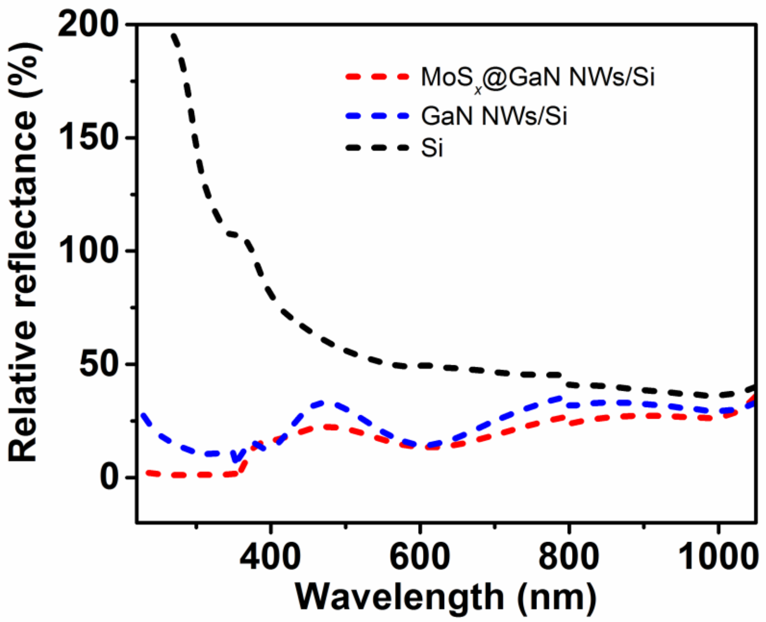


**Supplementary Figure 2 |** UV-Vis relative reflectance spectra of Si, GaN NWs/Si, and $MoS_x$@GaN NWs/Si measured under identical conditions.

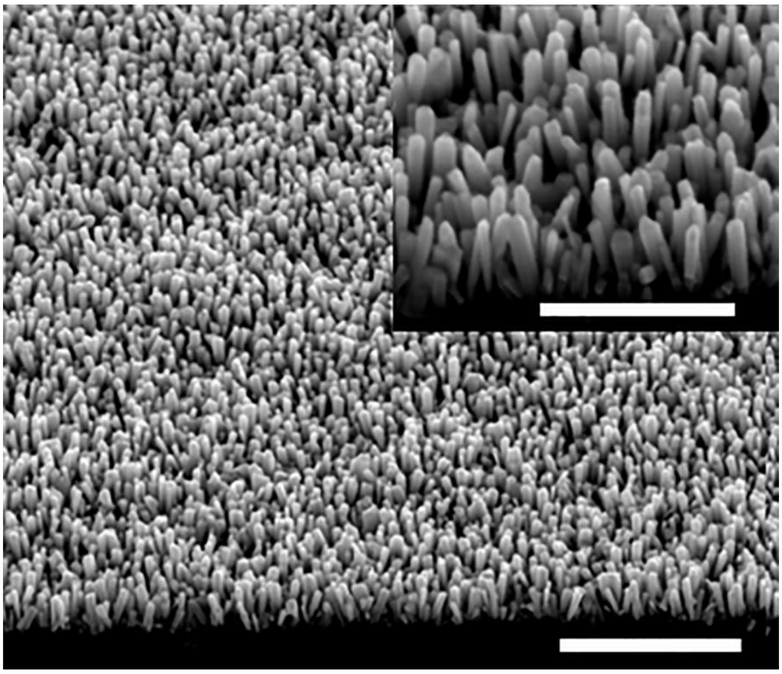

**Supplementary Figure 3 |** SEM image of GaN NWs/Si in the absence of $MoS_x$. Scale bar: 1 μm, inset 500 nm.

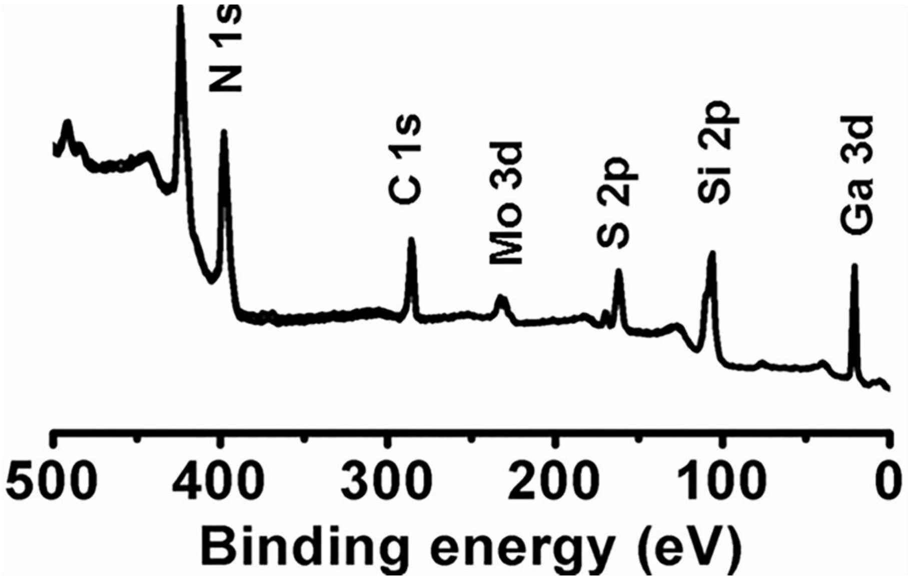


**Supplementary Figure 4 |** X-ray photoelectron spectrum of $MoS_x$@GaN NWs/Si.

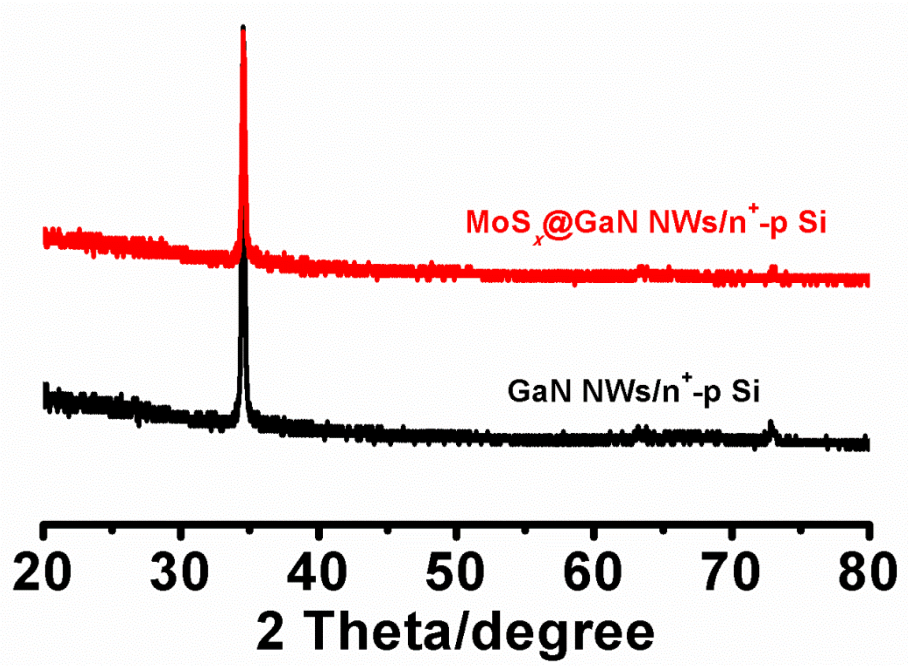


**Supplementary Figure 5 |** X-ray diffraction spectral of GaN NWs/Si and $MoS_x$@GaN NWs/Si.

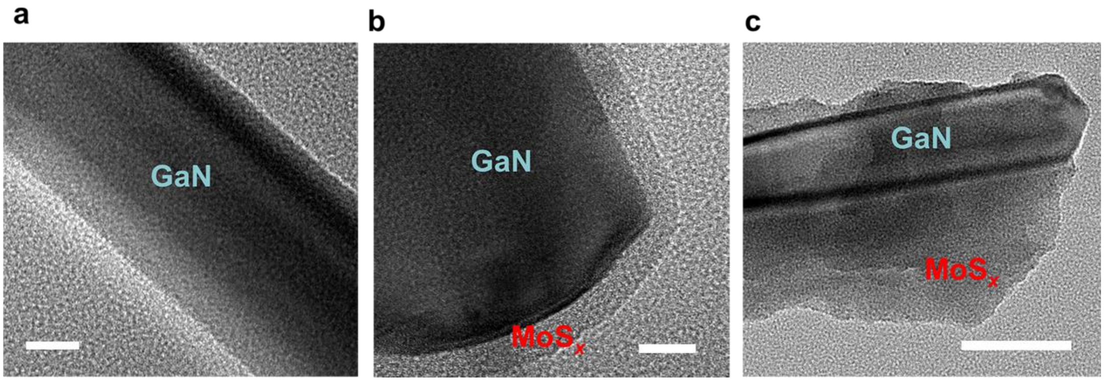


**Supplementary Figure 6 |** TEM images of GaN NWs/Si deposited with various densities of MoS$_x$. **a** 0 μmol cm$^{-2}$, **b** 0.73μmol cm$^{-2}$, and **c** 1.72μmol cm$^{-2}$. Scale bars: **a-b** 10 nm and **c** 50 nm

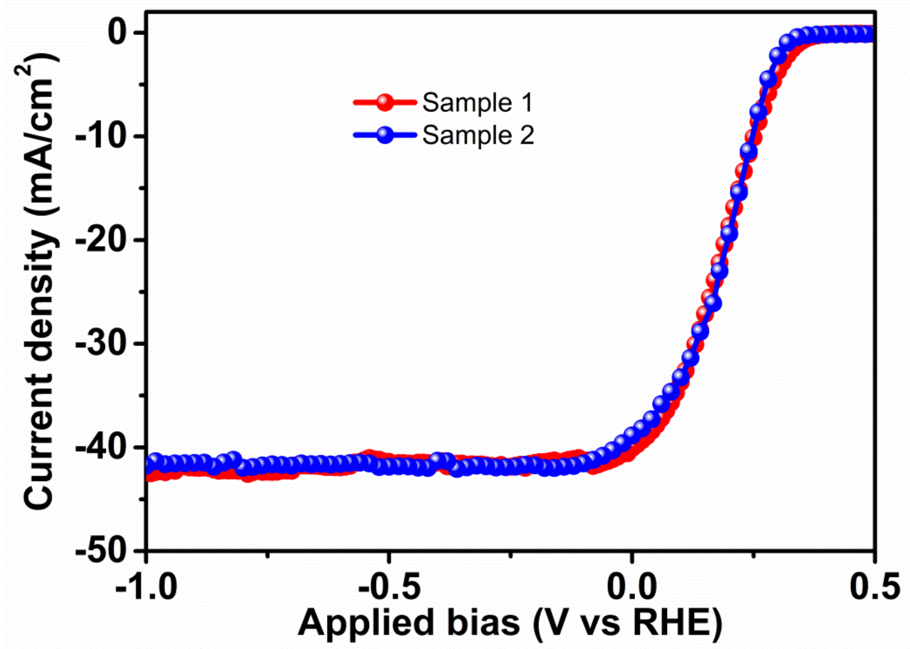


**Supplementary Figure 7 |** The variation of PEC performance of $MoS_x$@GaN NWs/Si with 0.73 μmol $cm^{-2}$ of $MoS_x$ under standard one-sun illumination in 0.5 M $H_2SO_4$.

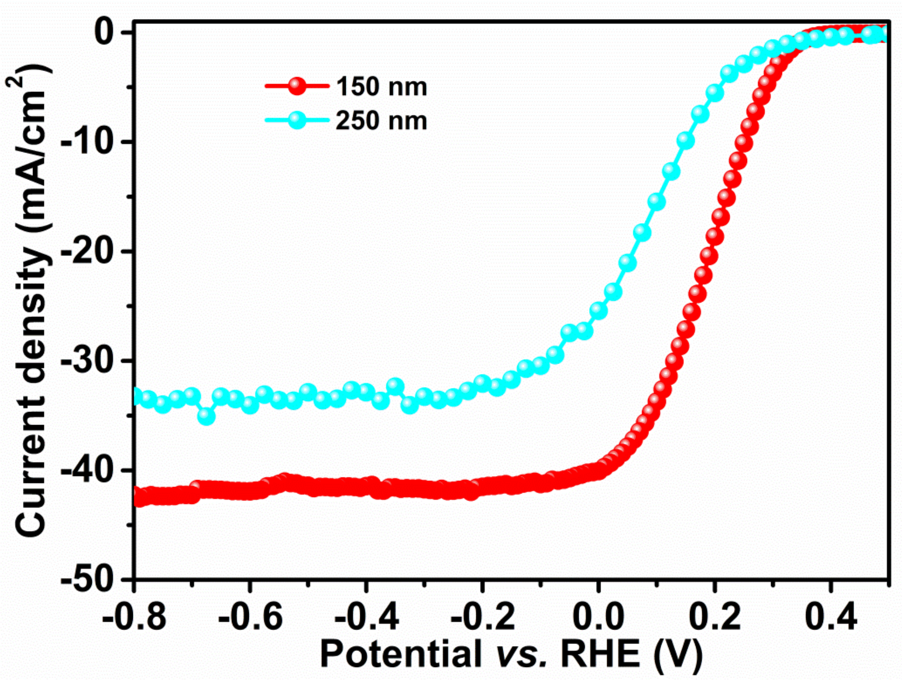


**Supplementary Figure 8 |** PEC performance of $MoS_x$@GaN NWs/Si with different lengths of GaN NWs.

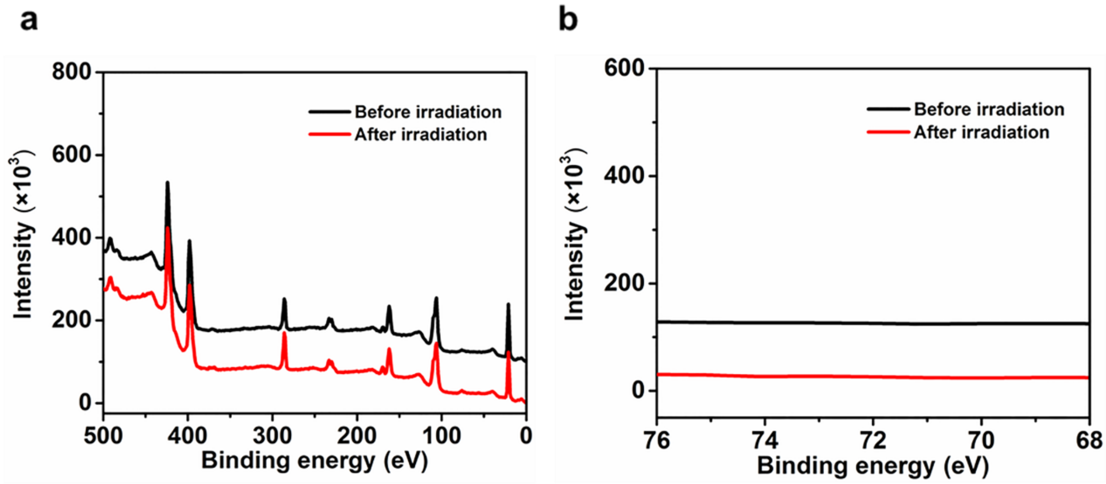


**Supplementary Figure 9** | X-ray photoelectron spectrum. **a** $MoS_x$@GaN NWs/Si and **b** the core level spectra of Pt 4f before and after 10 hours reaction under standard one-sun irradiation in 0.5 mol $L^{-1}$ $H_2SO_4$ aqueous solution.

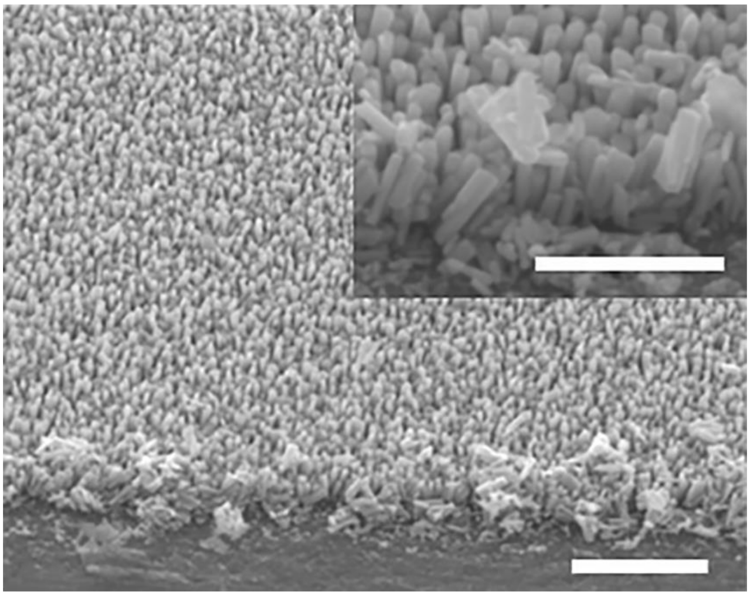

**Supplementary Figure 10 |** SEM image of $MoS_x$@GaN NWs/Si after 10 hours reaction under standard one-sun irradiation in 0.5 mol $L^{-1}$ $H_2SO_4$ aqueous solution. Scale bar: 2 μm, inset 500 nm.

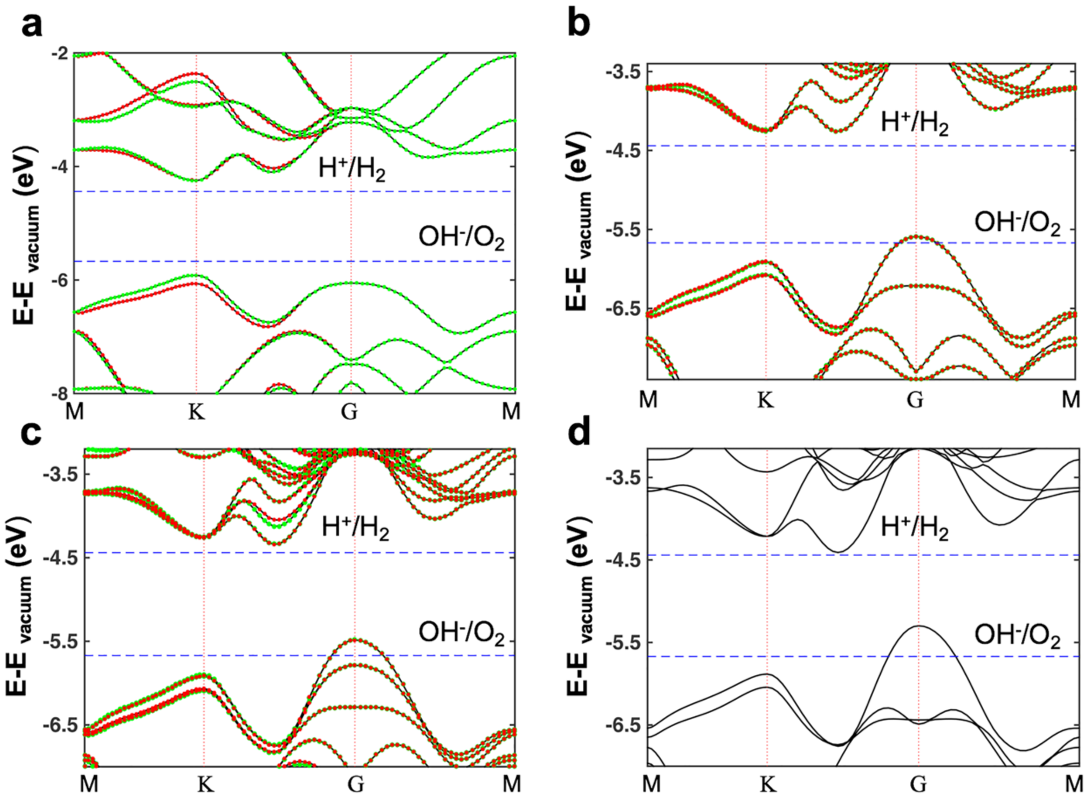


**Supplementary Figure 11 |** Band structure of $MoS_2$ with different thicknesses. **a** $MoS_2$-1L, **b** $MoS_2$-2L, **c** $MoS_2$-3L, **d** $MoS_2$-bulk. Spin-orbital coupling is taken into consideration for band structure calculations of few-layer $MoS_2$. In even-layer and bulk $MoS_2$, their inversion symmetry combined with time reversal leads to Kramers degeneracy, which means that no spin splitting exists. Oxidation-Reduction-Potential (ORP) is marked as $OH^-/O_2$ and $H^+/H_2$ with blue dashed line. This figure shows that regardless of the thickness of $MoS_2$, its conduction band minimum (CBM) remains at an optimal position referring to the reduction potential of $H_2O$ splitting.

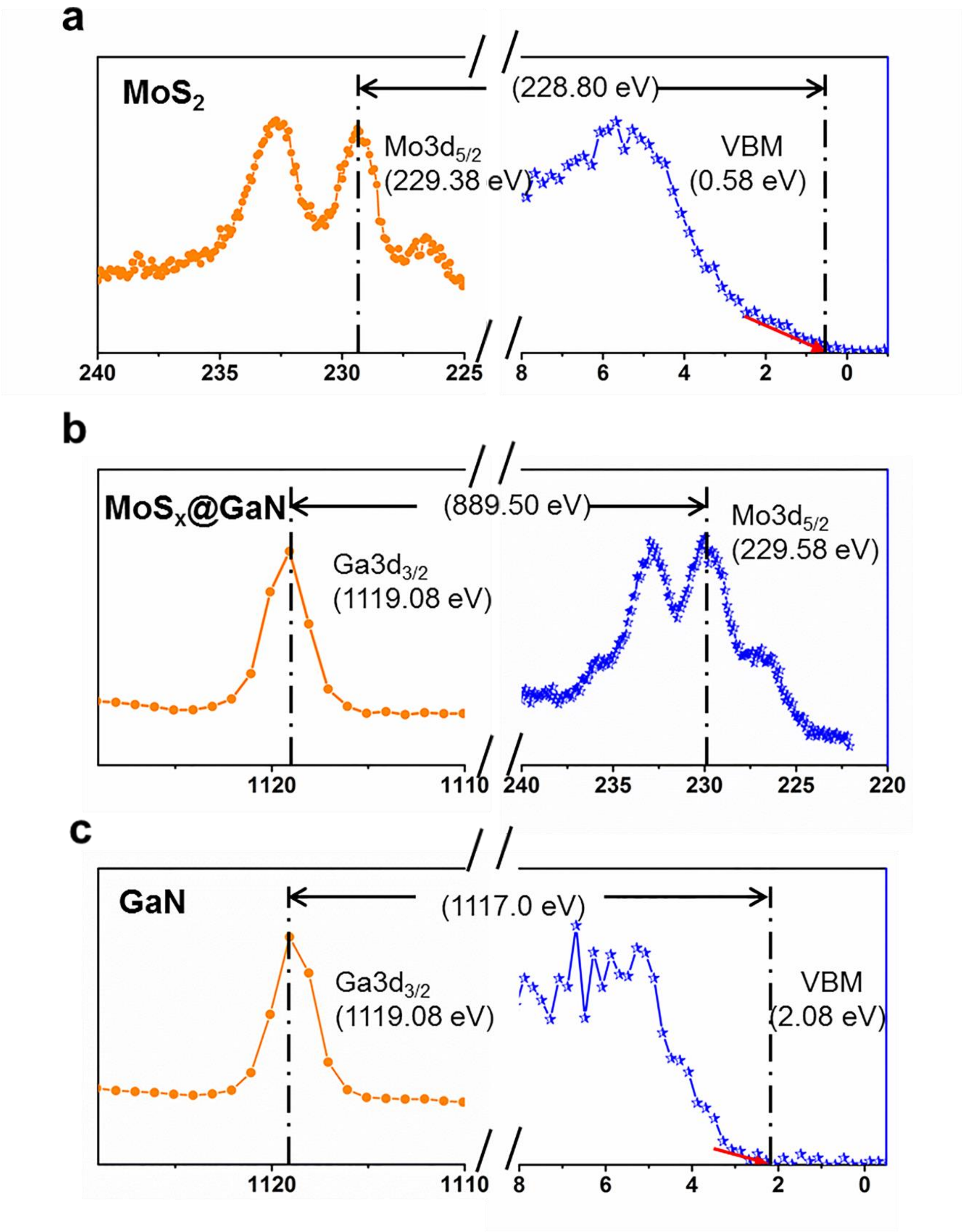


**Supplementary Figure 12 |** Core-level and valence band spectra based on XPS measurement. **a** $MoS_2$, **b** $MoS_x$@GaN, and **c** GaN.

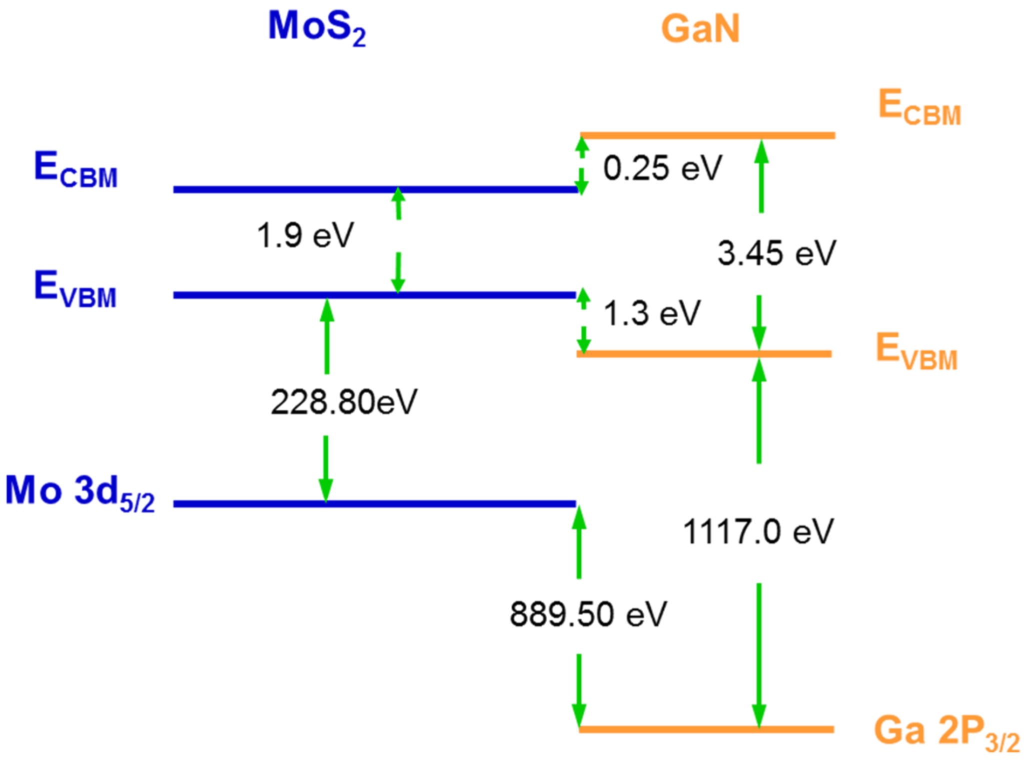


**Supplementary Figure 13 |** The flat band alignment diagram of $MoS_x$@GaN based on XPS measurement.

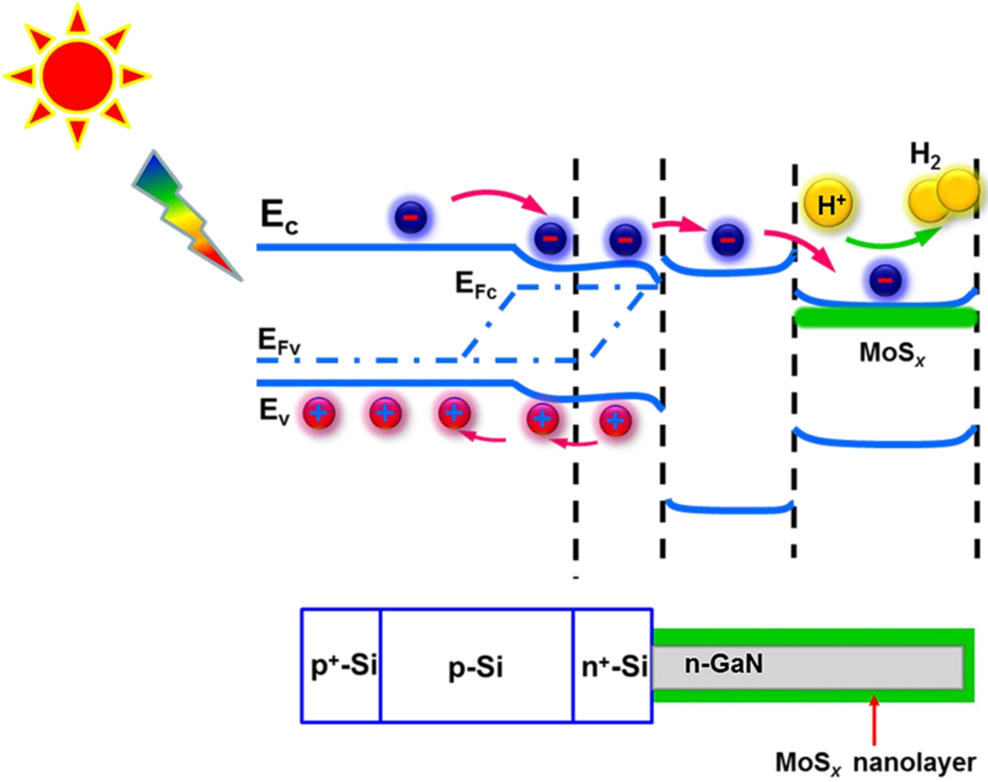


**Supplementary Figure 14 |** Energy band diagram of $MoS_x$@GaN NWs/Si under illumination. Herein, both Si and GaN are heavily n-type doped, which can facilitate the electrons transfer from Si to GaN. Moreover, under irradiation, the abundant photogenerated electrons result in flat-band condition, which decreases the upward bending of surface energy and promotes the electron injection from $n^+$-Si player to n-GaN at a small applied bias. The unique electronic interaction and outstanding geometric-matching structure between GaN and $MoS_2$ further provides an ideal electron-migration channel for the electrons transfer to HER catalytic sites.

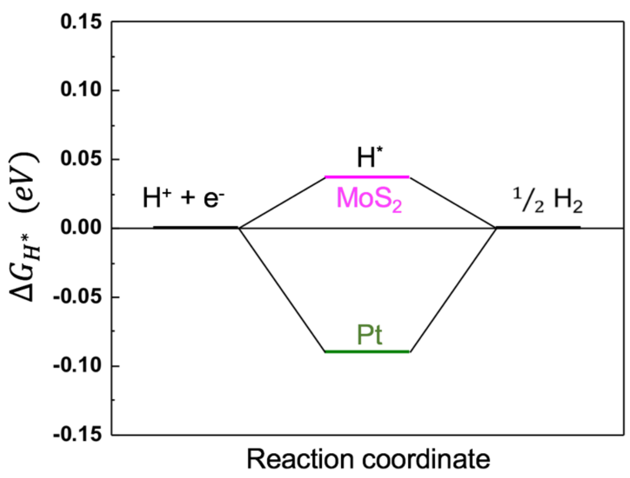


**Supplementary Figure 15 |** Free energy diagram of $MoS_2$ for HER at equilibrium (U=0) relative to SHE at pH = 0.

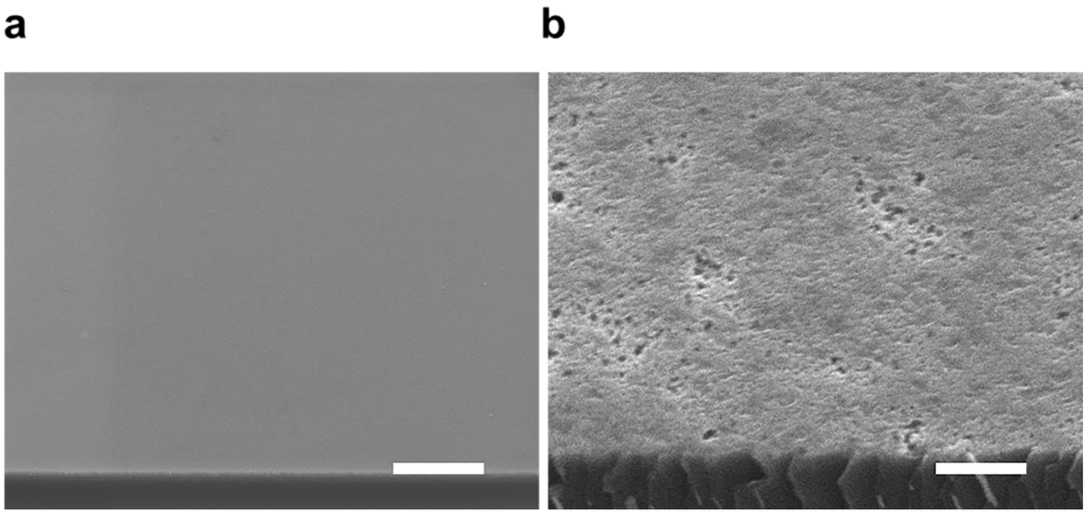


**Supplementary Figure 16 |** 45$^{o}$- titled SEM images. **a** bare planar $n^{+}$-p junction Si and **b** $MoS_x$/Si.

Scale bar: 1 μm.